Fluorescence Ultrasound Modulated Optical Tomography (fUMOT) in the Diffusive Regime

Yang Yang
Computational Math, Science and Engineering (CMSE)
Michigan State University

joint work with:
Wei Li, Louisiana State University
Yimin Zhong, University of California Irvine

Conference on Modern Challenges in Imaging: in the Footsteps of Allan MacLeod Cormack
MS1: Applied Math in Tomography, Tufts University August 5,

Outline

Optical Tomography

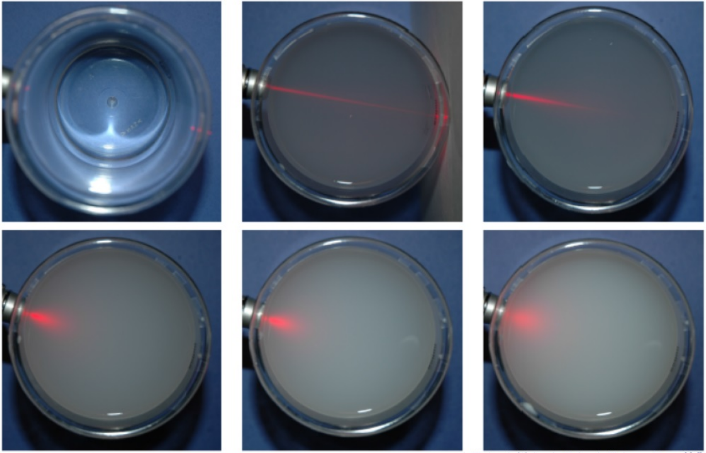

Figure: Credit: Nina Schotland

Fluorescence + Optical Tomography (fOT)

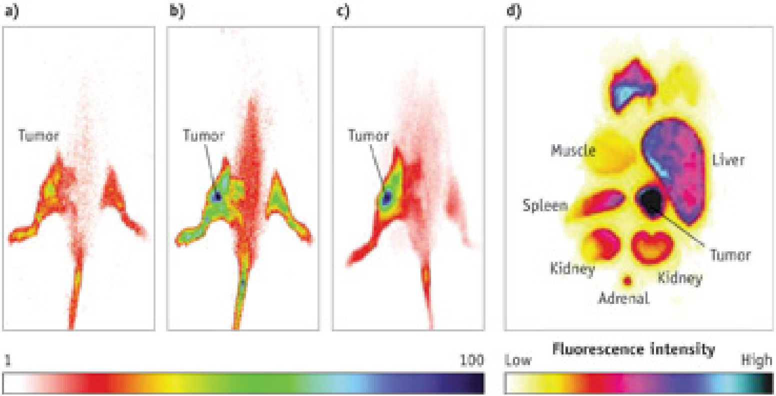

Figure: Fluorescence Optical Tomography (fOT). Image from Yang Pu et al, *"Cancer detection/fluorescence imaging: 'smart beacons' target cancer tumors"*, *BioOpticsWorld.com., 2013.*

Fluorescence + Ultrasound Modulation + Optical Tomography (fUMOT)

S: excitation light source, D: detector

solid curve: excitation photon path

dotted curve: emitted fluorescence photon path

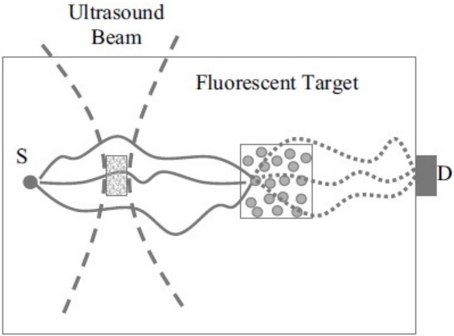

Figure: Fluorescence Ultrasound Modulated Optical Tomography (fUMOT). Image from B. Yuan et al, *"Mechanisms of the ultrasonic modulation of fluorescence in turbid media"*, *J. Appl. Phys. 2008; 104: 103102*

Incomplete literature

- **Fluorescence Optical Tomography (FOT)**: Arridge, Arridge-Schotland, Stefanov-Uhlmann, . . .
- **Ultrasound Modulated Optical Tomography (UMOT)**: Ammari-Bossy-Garnier-Nguyen-Seppecher, Bal, Bal-Moskow, Bal-Schotland, Chung-Schotland, . . .

Outline

fOT Model

Diffusive regime for fOT (Ren-Zhao 2013):

$u(\mathbf{x})$: excitation photon density, $w(\mathbf{x})$: emission photon density

fOT Model

Diffusive regime for fOT (Ren-Zhao 2013):

$u(\mathbf{x})$: excitation photon density, $w(\mathbf{x})$: emission photon density

- excitation process (subscripted by x):

$$\begin{cases} -\nabla \cdot D_x \nabla u + (\sigma_{x,a} + \sigma_{x,f})u = 0 & \text{in } \Omega \\ u = g & \text{on } \partial\Omega. \end{cases}$$

$D_x(\mathbf{x})$: diffusion coeffi. $g(\mathbf{x})$: boundary illumination

$\sigma_{x,a}(\mathbf{x})$: absorption coeffi. of medium $\sigma_{x,f}(\mathbf{x})$: absorption coeffi. of fluore

fOT Model

Diffusive regime for fOT (Ren-Zhao 2013):

$u(\mathbf{x})$: excitation photon density, $w(\mathbf{x})$: emission photon density

- excitation process (subscripted by x):

$$\begin{cases} -\nabla \cdot D_x \nabla u + (\sigma_{x,a} + \sigma_{x,f})u &= 0 \quad \text{in } \Omega \\ u &= g \quad \text{on } \partial\Omega. \end{cases}$$

$D_x(\mathbf{x})$: diffusion coeffi. $g(\mathbf{x})$: boundary illumination
$\sigma_{x,a}(\mathbf{x})$: absorption coeffi. of medium $\sigma_{x,f}(\mathbf{x})$: absorption coeffi. of fluore

- emission process (subscripted by m):

$$\begin{cases} -\nabla \cdot D_m \nabla w + (\sigma_{m,a} + \cancel{\sigma_{m,f}})w &= \eta\, \sigma_{x,f}\, u \quad \text{in } \Omega \\ w &= 0 \quad \text{on } \partial\Omega. \end{cases}$$

$D_m(\mathbf{x})$: diffusion coeffi. $\eta(\mathbf{x})$: quantum effciency coeffi.
$\sigma_{m,a}(\mathbf{x})$: absorption coeffi. of medium $\cancel{\sigma_{m,f}(\mathbf{x})}$: absorption coeffi. of fluor

Ultrasound Modulation Model

Ultrasound modulation with plane waves:

- weak acoustic field:

$$p(t, \mathbf{x}) = A\cos(\omega t)\cos(\mathbf{q}\cdot\mathbf{x} + \phi).$$

Ultrasound Modulation Model

Ultrasound modulation with plane waves:

- weak acoustic field:

$$p(t, \mathbf{x}) = A\cos(\omega t)\cos(\mathbf{q} \cdot \mathbf{x} + \phi).$$

- modulation effect on optical coefficients (Bal-Schotland 2009):

$$\begin{aligned}
D_x^\epsilon(\mathbf{x}) &= (1 + \epsilon\gamma_x \cos(\mathbf{q} \cdot \mathbf{x} + \phi))D_x(\mathbf{x}), & \gamma_x &= (2n_x - 1),\\
D_m^\epsilon(\mathbf{x}) &= (1 + \epsilon\gamma_m \cos(\mathbf{q} \cdot \mathbf{x} + \phi))D_m(\mathbf{x}), & \gamma_m &= (2n_m - 1),\\
\sigma_{x,a}^\epsilon(\mathbf{x}) &= (1 + \epsilon\beta_x \cos(\mathbf{q} \cdot \mathbf{x} + \phi))\sigma_{x,a}(\mathbf{x}), & \beta_x &= (2n_x + 1),\\
\sigma_{m,a}^\epsilon(\mathbf{x}) &= (1 + \epsilon\beta_m \cos(\mathbf{q} \cdot \mathbf{x} + \phi))\sigma_{m,a}(\mathbf{x}), & \beta_m &= (2n_m + 1),\\
\sigma_{x,f}^\epsilon(\mathbf{x}) &= (1 + \epsilon\beta_f \cos(\mathbf{q} \cdot \mathbf{x} + \phi))\sigma_{x,f}(\mathbf{x}), & \beta_f &= (2n_f + 1).
\end{aligned}$$

fUMOT Model

For $\epsilon > 0$ small,

- excitation process (subscripted by x):

$$\begin{cases} -\nabla \cdot D_x^\epsilon \nabla u^\epsilon + (\sigma_{x,a}^\epsilon + \sigma_{x,f}^\epsilon) u^\epsilon &= 0 \quad \text{in } \Omega \\ u^\epsilon &= g \quad \text{on } \partial\Omega. \end{cases}$$

- emission process (subscripted by m):

$$\begin{cases} -\nabla \cdot D_m^\epsilon \nabla w^\epsilon + (\sigma_{m,a}^\epsilon + \cancel{\sigma_{m,f}}) w^\epsilon &= \eta\, \sigma_{x,f}^\epsilon\, u^\epsilon \quad \text{in } \Omega \\ w^\epsilon &= 0 \quad \text{on } \partial\Omega. \end{cases}$$

fUMOT Model

For $\epsilon > 0$ small,

- excitation process (subscripted by x):

$$\begin{cases} -\nabla \cdot D_x^\epsilon \nabla u^\epsilon + (\sigma_{x,a}^\epsilon + \sigma_{x,f}^\epsilon) u^\epsilon & = & 0 & \text{in } \Omega \\ u^\epsilon & = & g & \text{on } \partial\Omega. \end{cases}$$

- emission process (subscripted by m):

$$\begin{cases} -\nabla \cdot D_m^\epsilon \nabla w^\epsilon + (\sigma_{m,a}^\epsilon + \cancel{\sigma_{m,f}}) w^\epsilon & = & \eta\, \sigma_{x,f}^\epsilon\, u^\epsilon & \text{in } \Omega \\ w^\epsilon & = & 0 & \text{on } \partial\Omega. \end{cases}$$

Meassurement: boundary photon currents $(D_x^\epsilon \partial_\nu u^\epsilon, D_x^\epsilon \partial_\nu w^\epsilon)|_{\partial\Omega}$.

fUMOT Model

For $\epsilon > 0$ small,

- excitation process (subscripted by x):

$$\begin{cases} -\nabla \cdot D_x^\epsilon \nabla u^\epsilon + (\sigma_{x,a}^\epsilon + \sigma_{x,f}^\epsilon) u^\epsilon = 0 & \text{in } \Omega \\ u^\epsilon = g & \text{on } \partial\Omega. \end{cases}$$

- emission process (subscripted by m):

$$\begin{cases} -\nabla \cdot D_m^\epsilon \nabla w^\epsilon + (\sigma_{m,a}^\epsilon + \cancel{\sigma_{m,f}}) w^\epsilon = \eta\, \sigma_{x,f}^\epsilon\, u^\epsilon & \text{in } \Omega \\ w^\epsilon = 0 & \text{on } \partial\Omega. \end{cases}$$

Meassurement: boundary photon currents $(D_x^\epsilon \partial_\nu u^\epsilon, D_x^\epsilon \partial_\nu w^\epsilon)|_{\partial\Omega}$.

Inverse Problem: recover $(\sigma_{x,f}, \eta)$.

fUMOT Model

For $\epsilon > 0$ small,

- excitation process (subscripted by x):

$$\begin{cases} -\nabla \cdot D_x^\epsilon \nabla u^\epsilon + (\sigma_{x,a}^\epsilon + \sigma_{x,f}^\epsilon) u^\epsilon &= 0 \quad \text{in } \Omega \\ u^\epsilon &= g \quad \text{on } \partial\Omega. \end{cases}$$

- emission process (subscripted by m):

$$\begin{cases} -\nabla \cdot D_m^\epsilon \nabla w^\epsilon + (\sigma_{m,a}^\epsilon + \cancel{\sigma_{m,f}}) w^\epsilon &= \eta\, \sigma_{x,f}^\epsilon\, u^\epsilon \quad \text{in } \Omega \\ w^\epsilon &= 0 \quad \text{on } \partial\Omega. \end{cases}$$

Meassurement: boundary photon currents $(D_x^\epsilon \partial_\nu u^\epsilon, D_x^\epsilon \partial_\nu w^\epsilon)|_{\partial\Omega}$.

Inverse Problem: recover $(\sigma_{x,f}, \eta)$.

Our strategy: recover $\sigma_{x,f}$ from the excitation process, then η from the emission process.

Outline

Derivation of Internal Data: I

For fixed boundary illumination g,

$$\int_\Omega (D_x^\epsilon - D_x^{-\epsilon})\nabla u^\epsilon \cdot \nabla u^{-\epsilon} + (\sigma_x^\epsilon - \sigma_x^{-\epsilon}) u^\epsilon u^{-\epsilon} d\mathbf{x} = \int_{\partial\Omega} (D_x^\epsilon \partial_\nu u^\epsilon) u^{-\epsilon} - (D_x^{-\epsilon} \partial_\nu u^{-\epsilon}) u$$

Derivation of Internal Data: I

For fixed boundary illumination g,

$$\int_\Omega (D_x^\epsilon - D_x^{-\epsilon})\nabla u^\epsilon \cdot \nabla u^{-\epsilon} + (\sigma_x^\epsilon - \sigma_x^{-\epsilon})u^\epsilon u^{-\epsilon} d\mathbf{x} = \int_{\partial\Omega} (D_x^\epsilon \partial_\nu u^\epsilon)u^{-\epsilon} - (D_x^{-\epsilon}\partial_\nu u^{-\epsilon})u$$

RHS is known. LHS has leading coefficient

$$J_1(\mathbf{q}, \phi) = \int_\Omega \left(\gamma_x D_x |\nabla u|^2 + (\beta_x \sigma_{x,a} + \beta_f \sigma_{x,f})|u|^2\right) \cos(\mathbf{q}\cdot\mathbf{x} + \phi) d\mathbf{x}.$$

Derivation of Internal Data: I

For fixed boundary illumination g,

$$\int_\Omega (D_x^\epsilon - D_x^{-\epsilon})\nabla u^\epsilon \cdot \nabla u^{-\epsilon} + (\sigma_x^\epsilon - \sigma_x^{-\epsilon}) u^\epsilon u^{-\epsilon} d\mathbf{x} = \int_{\partial\Omega} (D_x^\epsilon \partial_\nu u^\epsilon) u^{-\epsilon} - (D_x^{-\epsilon} \partial_\nu u^{-\epsilon}) u$$

RHS is known. LHS has leading coefficient

$$J_1(\mathbf{q}, \phi) = \int_\Omega \left(\gamma_x D_x |\nabla u|^2 + (\beta_x \sigma_{x,a} + \beta_f \sigma_{x,f})|u|^2\right) \cos(\mathbf{q}\cdot\mathbf{x} + \phi) d\mathbf{x}.$$

Varying $\mathbf{q}$ and ϕ gives the Fourier transform of

$$Q(\mathbf{x}) := \gamma_x D_x |\nabla u|^2 + (\beta_x \sigma_{x,a} + \beta_f \sigma_{x,f})|u|^2 \quad \text{in } \Omega,$$

where u is the unpertubed solution (i.e., $\epsilon = 0$).

Derivation of Internal Data: I

For fixed boundary illumination g,

$$\int_\Omega (D_x^\epsilon - D_x^{-\epsilon})\nabla u^\epsilon \cdot \nabla u^{-\epsilon} + (\sigma_x^\epsilon - \sigma_x^{-\epsilon}) u^\epsilon u^{-\epsilon} d\mathbf{x} = \int_{\partial\Omega} (D_x^\epsilon \partial_\nu u^\epsilon) u^{-\epsilon} - (D_x^{-\epsilon}\partial_\nu u^{-\epsilon}) u$$

RHS is known. LHS has leading coefficient

$$J_1(\mathbf{q}, \phi) = \int_\Omega \left(\gamma_x D_x |\nabla u|^2 + (\beta_x \sigma_{x,a} + \beta_f \sigma_{x,f})|u|^2\right) \cos(\mathbf{q}\cdot\mathbf{x} + \phi) d\mathbf{x}.$$

Varying $\mathbf{q}$ and ϕ gives the Fourier transform of

$$Q(\mathbf{x}) := \gamma_x D_x |\nabla u|^2 + (\beta_x \sigma_{x,a} + \beta_f \sigma_{x,f})|u|^2 \quad \text{in } \Omega,$$

where u is the unpertubed solution (i.e., $\epsilon = 0$).

Observation: if u can be recovered from Q, so can $\sigma_{x,f}$.

Inverse Problems Recast

Inverse Problem Recast: recover u from Q.

Recall

$$\begin{cases} -\nabla \cdot D_x \nabla u + (\sigma_{x,a} + \sigma_{x,f})u & = & 0 & \text{in } \Omega \\ u & = & g & \text{on } \partial\Omega. \end{cases}$$

and the internal data is

$$Q(\mathbf{x}) := \gamma_x D_x |\nabla u|^2 + (\beta_x \sigma_{x,a} + \beta_f \sigma_{x,f})|u|^2 \quad \text{in } \Omega.$$

Inverse Problems Recast

Inverse Problem Recast: recover u from Q.

Recall

$$\begin{cases} -\nabla \cdot D_x \nabla u + (\sigma_{x,a} + \sigma_{x,f})u = 0 & \text{in } \Omega \\ u = g & \text{on } \partial\Omega. \end{cases}$$

and the internal data is

$$Q(\mathbf{x}) := \gamma_x D_x |\nabla u|^2 + (\beta_x \sigma_{x,a} + \beta_f \sigma_{x,f})|u|^2 \quad \text{in } \Omega.$$

- $\beta_f = 0$: solving a Hamilton-Jacobi equation to find u;
- $\beta_f \neq 0$: eliminating $\sigma_{x,f}$ through substitution.

Recovery of $\sigma_{x,f}$: uniqueness

- $\beta_f \neq 0$ (conti.ed):

set $\theta := \frac{\beta_f - \gamma_x}{\beta_f + \gamma_x}$ and $\Psi := u^{\frac{2}{1+\theta}}$

$$\begin{cases} \nabla \cdot D_x \nabla \Psi &= \underbrace{-\frac{2}{1+\theta}\sigma_{x,a}\left(\frac{\beta_x}{\beta_f} - 1\right)}_{:=b} \Psi + \underbrace{\frac{2}{1+\theta}\frac{Q}{\beta_f}}_{:=c} |\Psi|^{-(1+\theta)}\Psi \\ \Psi &= g^{\frac{2}{1+\theta}} \end{cases}$$

Theorem (Li-Y.-Zhong, 2018)

The semi-linear elliptic BVP has a unique positive weak solution $\Psi \in H^1(\Omega)$ in either of the following cases:

Case (1): $-1 \neq \theta < 0$, $b \geq 0$ *and* $c \geq 0$;

Case (2): $\theta \geq 0$, $b \geq 0$ *and* $c \leq 0$.

Recovery of $\sigma_{x,f}$: stability and reconstruction

Theorem (Li-Y.-Zhong, 2018)

In either Case (1) or Case (2), one has the stability estimate

$$\|\sigma_{x,f} - \tilde{\sigma}_{x,f}\|_{L^1(\Omega)} \leq C\left(\|Q - \tilde{Q}\|_{L^1(\Omega)} + \|Q - \tilde{Q}\|^2_{L^2(\Omega)}\right)$$

We further give three iterative algorithms with convergence proofs to reconstruct $\sigma_{x,f}$.

Remark: uniqueness and stability may fail if θ, b, c violate the conditions.

Recovery of η

Sketch of procedures:

1. derive an integral identity from the emission process;

Recovery of η

Sketch of procedures:

1. derive an integral identity from the emission process;
2. derive an internal functional S from the leading order term of the identity;

Recovery of η

Sketch of procedures:

1. derive an integral identity from the emission process;
2. derive an internal functional S from the leading order term of the identity;
3. rewrite the equations for u and w to obtain a Fredholm type equation
$$\mathcal{T}\eta = S;$$

Recovery of η

Sketch of procedures:

1. derive an integral identity from the emission process;
2. derive an internal functional S from the leading order term of the identity;
3. rewrite the equations for u and w to obtain a Fredholm type equation
$$\mathcal{T}\eta = S;$$
4. if 0 is not an eigenvalue of $\mathcal{T}$, then uniqueness, stability and reconstruction are immediate.

Numerical examples

Domain: $[-0.5, 0.5]^2$; excitation source: $g(x, y) = e^{2x} + e^{-2y}$..

The domain is triangulated into 37008 triangles and uses 4-th order Lagrange finite element method to solve the equations.

$$D_x \equiv 0.1, \qquad D_m = 0.1 + 0.02\cos(2x)\cos(2y),$$
$$\sigma_{x,a} \equiv 0.1, \qquad \sigma_{m,a} = 0.1 + 0.02\cos(4x^2 + 4y^2).$$

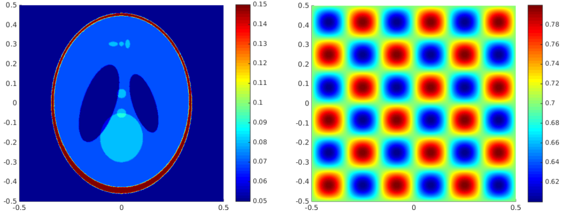

Figure: Left: The absorption coefficient $\sigma_{x,f}$ of fluorophores. Right: The quantum efficiency coefficient η.

Numerical examples- Case I-1

$\gamma_x = -2.6$, $\gamma_m = -2.4$, $\beta_x = -0.6$, $\beta_m = -0.4$, $\beta_f = -0.8$ and $\tau = 3.25$. $\mu = -0.25$ and $\theta = -\frac{9}{17}$.

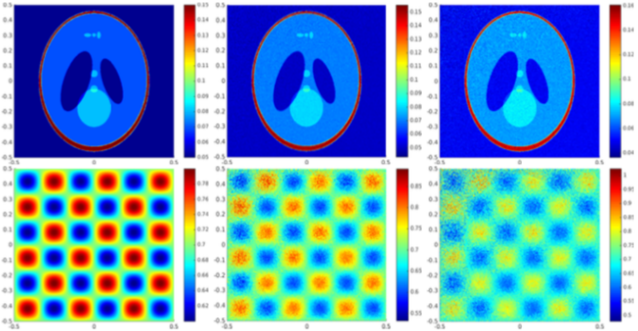

Figure 2: The reconstruction of $\sigma_{x,f}$ and η in Example I. First row, from left to right, 0%, 1%, 2% random noises are added to the internal data Q and the relative L^1 errors of reconstructed $\sigma_{x,f}$ are 0.000132%, 3.88%, 7.76% respectively. Second row, from left to right, assuming the knowledge of $\sigma_{x,f}$ from the first row, 0%, 1%, 2% random noises are added to the internal data S. The relative L^2 errors of reconstructed η are 0.00313%, 5.60%, 11.7% respectively.

Numerical examples- Case I-2

$\gamma_x = -1.4$, $\gamma_m = 0.0$, $\beta_x = 0.6$, $\beta_m = 2.0$, $\beta_f = 0.4$ and $\tau = -3.5$.
$\mu = 0.5$ and $\theta = -\frac{9}{5}$.

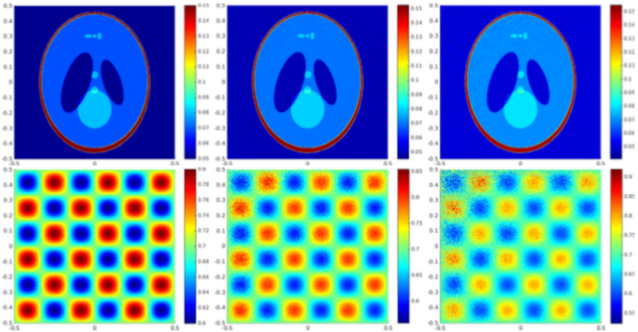

Figure 3: The reconstruction of $\sigma_{x,f}$ and η in Example II. First row, from left to right, 0%, 1%, 2% random noises are added to the internal data Q and the relative L^1 errors of reconstructed $\sigma_{x,f}$ are 0.0086%, 2.62%, 5.27% respectively. Second row, from left to right, assuming the knowledge of $\sigma_{x,f}$ from the first row, 0%, 1%, 2% random noises are added to the internal data S. The relative L^2 errors of reconstructed η are 0.0150%, 4.23%, 8.89% respectively.

Numerical examples- Case II

$\gamma_x = 0.2$, $\gamma_m = 0.6$,, $\beta_x = 2.2$, $\beta_m = 2.6$, $\beta_f = -0.3$ and $\tau = -\frac{2}{3}$. $\mu = -\frac{25}{8}$ and $\theta = 5$.

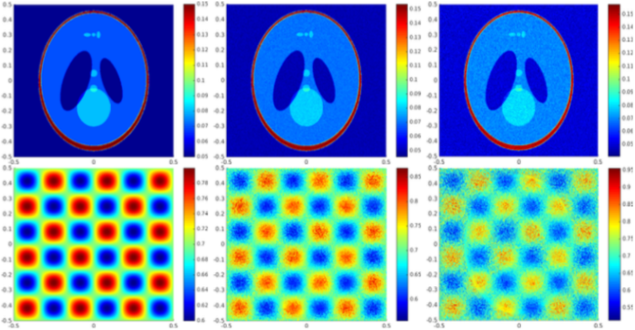

Figure 4: The reconstruction of $\sigma_{x,f}$ and η in Example III. First row, from left to right, 0%, 1%, 2% random noises are added to the internal data Q and the relative L^1 errors of reconstructed $\sigma_{x,f}$ are 0.00147%, 3.68%, 7.38% respectively. Second row, from left to right, assuming the knowledge of $\sigma_{x,f}$ from the first row, 0%, 1%, 2% random noises are added to the internal data S. The relative L^2 errors of reconstructed η are 0.00392%, 4.65%, 9.48% respectively.

Thank you for the attention!

Research partly supported by NSF grant DMS-1715178